Research on Biomedical Engineering
rbejournal.org
Volume 32, Number 2, p. 129-136, 2016

Original Article
DOI: http://dx.doi.org/10.1590/2446-4740.00315

Reticular pattern detection in dermoscopy: an approach using Curvelet Transform

Marlene Machado, Jorge Pereira, Rui Fonseca-Pinto*

Abstract **Introduction**: Dermoscopy is a non-invasive in vivo imaging technique, used in dermatology in feature identification, among pigmented melanocytic neoplasms, from suspicious skin lesions. Often, in the skin exam is possible to ascertain markers, whose identification and proper characterization is difficult, even when it is used a magnifying lens and a source of light. Dermoscopic images are thus a challenging source of a wide range of digital features, frequently with clinical correlation. Among these markers, one of particular interest to diagnosis in skin evaluation is the reticular pattern. **Methods**: This paper presents a novel approach (avoiding pre-processing, e.g. segmentation and filtering) for reticular pattern detection in dermoscopic images, using texture spectral analysis. The proposed methodology involves a Curvelet Transform procedure to identify features. **Results**: Feature extraction is applied to identify a set of discriminant characteristics in the reticular pattern, and it is also employed in the automatic classification task. The results obtained are encouraging, presenting Sensitivity and Specificity of 82.35% and 76.79%, respectively. **Conclusions**: These results highlight the use of automatic classification, in the context of artificial intelligence, within a computer-aided diagnosis strategy, as a strong tool to help the human decision making task in clinical practice. Moreover, the results were obtained using images from three different sources, without previous lesion segmentation, achieving to a rapid, robust and low complexity methodology. These properties boost the presented approach to be easily used in clinical practice as an aid to the diagnostic process.

Keywords: Curvelet Transform, Dermoscopy, Reticular pattern, Melanoma, Pattern recognition.

Introduction

Malignant melanoma is the most aggressive and the deadliest form of skin cancer among the Caucasian population (Longo et al., 2012). The United States epidemiology of cancer, laid skin cancer as the most common form of malignancy over the past three decades (Rogers et al., 2010; Stern, 2010). In particular, melanoma is the most common form of cancer in young adults (25-29 years old), and the second most common form of cancer affecting young people (15-29 years old) (Bleyer et al., 2006). In Europe, several studies have documented increase of melanoma incidence in the last few decades (Baumert et al., 2009; Downing et al., 2006; Sant et al., 2009). In the particular case of Portugal, where the sun exposure is high, the estimated incidence for 2012 was 7.5 per 100 000, mortality 1.6 per 100 000 and prevalence at one, three and five years 12.08%, 33.99% and 53.93% respectively (Ferlay et al., 2013). Due to the increase in incidence (Downing et al., 2006; Ferlay et al., 2013) and the consequent increase in mortality, malignant melanoma represents a significant and growing public health problem (Longo et al., 2012). Therefore, the earlier detection of melanoma is essential, and is still one of the most challenging problems in dermatology.

Dermoscopy is a non-invasive imaging technique used to obtain digital images on the surface of the skin, and it has been successfully applied since early 90 of the last century (Benelli et al., 1999; Fonseca-Pinto et al., 2010; Menzies et al., 1996; Soyer et al., 1995).

Clinical diagnosis of cutaneous melanoma is commonly based on the ABCD rule (Friedman et al., 1985), Menzies method (Menzies, 2001) and seven-point checklist (Liu et al., 2005). According to the above-cited methods, melanomas usually have differential structures, such pigmented networks, streaks or dots, giving clues about their melanocytic origin. The pigmented network is an important diagnostic clue, representing a dermoscopic hallmark of melanocytic lesions, which presence is, in general, independent of the presence or absence of a carcinogenic process. The reticular pattern appears as a grid of thin brown lines, over a diffuse light brown background. This is a honeycomb-like structure, consisting of round-pigmented lines and lighter hypo-pigmented

*e-mail: rui.pinto@ipleiria.pt
Received: 24 July 2015 / Accepted: 19 June 2016

holes, forming a subtle pattern that appears in many melanocytic lesions. This pigment distribution is arranged in keratinocytes or along the dermoepidermal junction along the rete-ridge, forming the observed pattern at the outer layer of the skin.

The importance of early detection in skin cancer, and the complexity of the clinical decision regarding the nature of the lesion, led in the last decade the appearance of several works on the automatic detection of pigmented network, whose contribution is very useful to enhance medical classification by dermatologists. In these works, most of the algorithms carry out an automatic segmentation of the lesion, followed by the calculation of features such as color, texture and shape characteristics. In the following, an automatic learning algorithm is applied to select the most discriminant features, enabling the automatic classification (Anantha et al., 2004; Arroyo and Zapirain, 2014; Barata et al., 2012; Betta et al., 2006; Fleming et al., 1998; Grana et al., 2006; Leo et al., 2010; Sadeghi et al., 2011).

The automated detection of the reticular pattern or pigment network is often a challenging problem, since in these reticular structures there is a low contrast between the network and the background, the size of net holes may comprise different sizes in different images, and also, in the same image often exists irregularities in their shape and size.

The main objective within this work is to present a robust, rapid, and low complexity system, to identify the presence of reticular pattern in dermoscopic images, avoiding the standard previous preprocessing steps (lesion segmentation, filtering, artifact removal, …), suitable for usage with different dermoscopic acquisition systems.

Methods

Color and texture features are the two main groups of image characteristics, used by dermatologists, to differentiate skin melanocytic patterns. Local dermoscopic structures, such as reticular pattern, can be described by texture features, whereas these markers denote spatial intensities in an image, enabling the identification of different shapes.

Texture is a commonly used tool in the analysis and interpretation of images. There are two main approaches in texture feature extraction, accordingly to the division among spatial or spectral domain methodologies (Sumana, 2008). Spectral approaches, as in Wavelet and Curvelet Transforms, are more robust to noise than the spatial approaches such as Co-Occurrence matrices, Laws filters, edge histogram, etc. Therefore, spectral approaches are widely used for texture feature extraction, from image compression to image de-noising and classification (Calderbank et al., 1997; Eltoukhy et al., 2010; Starck et al., 2002).

The Wavelet theory has been broadly used for texture classification. The success of Wavelets is owing to the driven performance in one-dimensional pricewise smooth functions, detecting singularities (points) (Do and Vetterli, 2003). However, images generally include 1D singularity structures (edges and corners), thus its use in images are of restricted use.

To overcome the weakness of the Wavelets on traditional multi-scale representations, and to capture other directional features, the Curvelet transform has emerged as a new multi-resolution analysis tool. Curvelet analysis was first proposed by Candès et al. (2006), and it is known as the first generation Curvelet transform. Some studies have been developed with Curvelets in biomedical imaging such mammogram images (Eltoukhy et al., 2010; Gardezi et al., 2014), endoscopy images (Li and Meng, 2009) or fingerprint images (Nikam and Agarwal, 2008).

In this study, skin lesions are classified based on image texture features using the Curvelet transform. The classification approach consists of two main processing steps. First, the Curvelet transform is applied on a set of dermoscopy images, and a set of statistical features (mean, standard deviation, energy, entropy and homogeneity) are extracted from each of the Curvelets sub-bands. Next, a classifier/feature selector is built using the AdaBoost learning algorithm, adapted from Viola and Jones (2004). This approach will select the best features to discriminate between lesions with reticular pattern and lesions without reticular pattern, and to assign probabilities of being lesion with reticular pattern.

Image preprocessing

In contrast to other methodologies in the context of dermoscopic machine learning algorithms, the process of detecting and removing artifacts, and the previous segmentation were not followed within the proposed methodology. As a preprocessing step, the conversion from RGB into a gray-level image was performed by selecting the highest entropy channel. Next, an image cropping operation was conducted, reducing by this way the background interference. In fact, in the original images, 30 to 50% of the image size is composed by background pixels, contributing for noise. After this cropping step, the image is resized into a fixed size of 512×512. In the results we put forward in this work, this task was manually made, however it can be automatically performed, by align all images using the centroid, and then define the length of the cropping operator. In fact, right now,

this procedure is implemented, and it is running in our current studies. An example of the cropping process output is shown in Figure 1.

Curvelet Transform

The Wavelet transform appears as a mathematical strategy to decompose an image into a scale-frequency domain representation, which can further be divided into sub-band images of different frequency components. Each component is analyzed with a resolution matching its scale. Wavelet transform has advantages over traditional Fourier methods in analyzing physical situations where the signal contains discontinuities and sharp spikes. However, despite the Wavelet transform ability for horizontal, vertical and diagonal detail extraction, these three directions, in general, do not provide enough information among other directions. This limitation can be of particular importance in feature extraction in dermoscopy, since the growing path of melanocytic lesions does not obey to strict geometric rules.

To improve the performance of image details extraction, Candès (1998) proposed the use of the Ridgelet Transform. Ridgelets are based on tracking a line into a point singularity, by using the Radon Transform. In fact, point singularity in the Radon domain can be handled by using the Wavelet transform. Thus, Ridgelet Transform is more efficient in representing edges and other singularities along lines than Wavelets, as noted in Do and Vetterli (2003).

Images contain edges, which are typically more curved than straight. Therefore, Ridgelets alone cannot represent such curves efficiently. However, one curved edge can be viewed as a straight line at a sufficient fine scale. Thus, to compute curved edges, Ridgelets can be applied based on a local approach. Hence, Candès et al. (2006) emerged with the idea behind the Curvelet Transform by segmenting curves into a set of fragments, and then use Ridgelet Transform to represent each ridge piece.

The discrete Curvelet transform of a continuum function *f(x1, x2)* uses a dyadic sequence of scales, and a filter bank $(P_0 f, \Delta_1 f, \Delta_2 f, \ldots)$, where the passband filter Δ_s is concentrated in the proximity of the frequencies $[2^{2s}, 2^{2s+2}]$. In wavelet theory, the decomposition is performed into dyadic sub-bands $[2^{2s}, 2^{2s+1}]$, in contrast, the sub-bands used in the discrete Curvelet Transform have the nonstandard form $[2^{2s}, 2^{2s+2}]$. Implementation of the Curvelet Transform is settled by the next definitions and steps:

- *Sub-band Decomposition:* The image f is decomposed into sub-bands, according to Equation 1,

$$f \mapsto (P_0 f, \Delta_1 f, \Delta_2 f, \ldots) \quad (1)$$

where P_0 represents a low pass filter.

- *Smooth Partitioning*: A grid of a dyadic squares is define as $Q_{(s,k_1,k_2)} \left[\frac{k_1}{2^s}, \frac{k_1+1}{2^s}\right] \times \left[\frac{k_2}{2^s}, \frac{k_2+1}{2^s}\right]$

and thus, each sub-band is smoothly windowed into "squares" of an appropriate scale (of side length ~ 2^{-s}) defined in Equation 2,

$$\Delta_s f \mapsto (w_Q \Delta_s f)_{Q \in Q_s} \quad (2)$$

where W_Q is a smooth windowing function in the vicinity of Q, with main support size $2^{-s} \times 2^{-s}$.

- *Renormalization*: The resulting squares are renormalized to unit scale as presented in Equation 3,

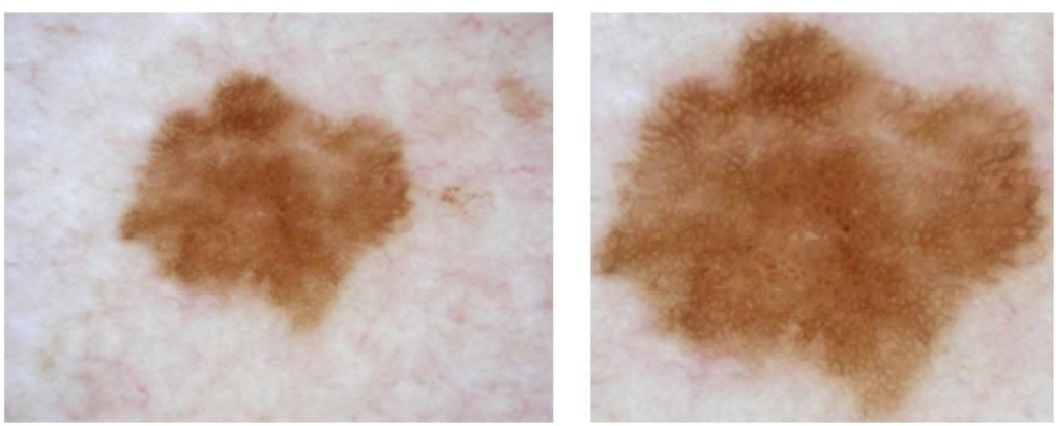

Figure 1. Left - Original image; Right - Cropped image.

$$g_Q = (T_Q)^{-1}(w_Q \Delta_s f), \qquad Q \in Q_s \tag{3}$$

where T_Q is defined, for each Q as

$T_Q f(x,y) = 2^s f(2^s x - k_1, 2^s y - k_2)$.

- *Ridgelet Analysis*: Ridgelet transform (Candès, 1998) is performed on each renormalized square. The block diagram for the implementation of digital Ridgelet Transform is shown in Figure 2.

In this definition, the two dyadic sub-bands $[2^{2s}, 2^{2s+1}]$ and $[2^{2s+1}, 2^{2s+2}]$ are merged, and then the Ridgelet Transform is applied.

Feature extraction, feature selection and classification

Regarding feature selection task, the *CuvLab toolbox* (Candès et al., 2006) was used, and two commonly used Curvelet Transforms were tested (the Unequally-Spaced Fast Fourier Transform (USFFT) and wrapping based fast Curvelet Transform (WFCT)). Contrary to Fadili and Starck (2007), this work put forward improved results when using USFFT (concerning Specificity, Sensitivity and Accuracy). For the image decomposition step, several scales of decomposition were tested to obtain the Curvelet coefficients. The best result was obtained with nine scales.

Statistical features such as mean (μ), standard deviation (σ), energy (e), entropy (E) and homogeneity (*H*) were calculated from each Curvelet sub-band, and they were used to construct four global feature vectors as $F1 = [F_\mu, F_\sigma, F_e, F_E]$, $F2 = [F_\sigma, F_e, F_E]$, $F3 = [F_\sigma, F_E]$ and $F4 = [F_\sigma, F_e, F_E, F_H]$, where $F_\mu = [\mu_1, \mu_2, ..., \mu_s]$, $F_\sigma = [\sigma_1, \sigma_2, ..., \sigma_s]$, $F_e = [e_1, e_2, ..., es]$, $F_E = [E_1, E_2, ..., E_s]$ and $F_H = [H_1, H_2, ..., H_s]$. In the construction of the four global feature composition, all combinations were tested and the configuration was elicited by selecting the high score combinations (Table 1).

For the construction of the training model, 70 images obtained from the *Derm101* [derm01] and *PCDS* databases [pcds], were used. The AdaBoost algorithm as adapted form Viola and Jones (2004) was chosen for the automatic classification, as it simultaneously selects the best features and trains the classifier. Generally, the AdaBoost classifier selects a small subset from the initial set, called weak classifiers, and combines the selected algorithms into a strong, well-performing classifier. For more details, regarding the boosting technique, please see the reference where the methodology where originality presented in (Paradiso and Carney, 1988). The variant of the AdaBoost algorithm used in this paper identifies weak classifiers with texture features.

Results

In this section, a summary of the conducted experiments and obtained results is presented.

Dataset

To evaluate the discrimination power of the proposed spectral textural feature characterization, a set of extensive experiments it was conducted, by using images from three different certified databases: *Derm101* [derm01], *Hosei Dataset* [zhou] and *PCDS Database* [pcds]. These images were obtained by dermatologists during clinical exams. All images were stored in *JPEG* formats. From these databases, three different datasets containing 90, 53, and 15 RGB images where used, respectively. Regarding image resolution, the 90 images from [derm01] have 600×650. For the other two sets, image resolution was not constant, ranging from 600×550 till 900×900. Each image was cropped and resized for 512×512 to avoid unnecessary background information, increasing by this way the signal to noise ratio.

For training and validation purposes, each image was labeled as *with* or *without reticular pattern* (ground truth label).

Table 1. Classification results.

Feature type	SE (%)	SP (%)	Q (%)	Classifier parameter
F1	66.99	71.43	68.55	K=8
F2	**82.35**	**76.79**	**80.38**	**K=100**
F3	76.70	69.64	74.21	K=120
F4	72.82	71.43	72.33	K=8

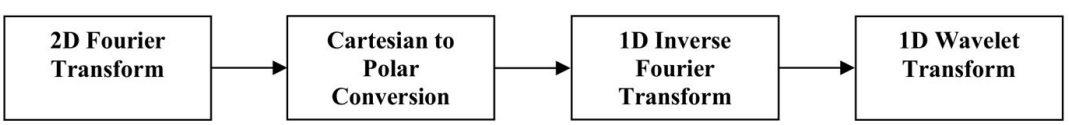

Figure 2. Ridgelet transform diagram.

Evaluation metrics and results

To test the performance of the proposed methodology, common evaluation metrics were used, i.e, Sensitivity (*SE*), Specificity (*SP*) and Accuracy (*Q*).

The four features set *(F1, F2, F3* and *F4),* were tested independently and evaluated on all the sub-bands, totalizing 936, 720, 468 and 936 features, respectively. In Table 1 it is possible to observe the feature combination for the lesion classification. The F2 feature set reached superior performance achieving *SE* = 82.35% and *SP* = 76.79%.

Although the obtained results were encouraging, there are some demanding images where the detector flops. In Figure 3 it is possible to observe (top left and top right) several dots and dark circular structures, functioning as a confounding factor, and this texture pattern is falsely detected by the algorithm, although it is not a reticular pattern. Likewise, in bottom-left and bottom-right, there are lesions with reticular pattern, but they were wrongly labeled as not having it. To overcome this problem, additional information is needed to increase the classification accuracy. This additional information, in terms of extracted features must joint other pattern analysis obtained from the image (e.g. fissures and comedo-like openings, cobblestone pattern, peripheral and eccentric globules, etc…).

Discussion

The use of automatic classification in dermoscopy is a strong tool to access dermatologists in clinical diagnosis, in the major challenge of the early detection of skin cancer. Skin lesion classification is based on the identification of structures, whose features allow the quantification using of well-known classification rules (ABCD, Menzies method, 7 point check-list, …).

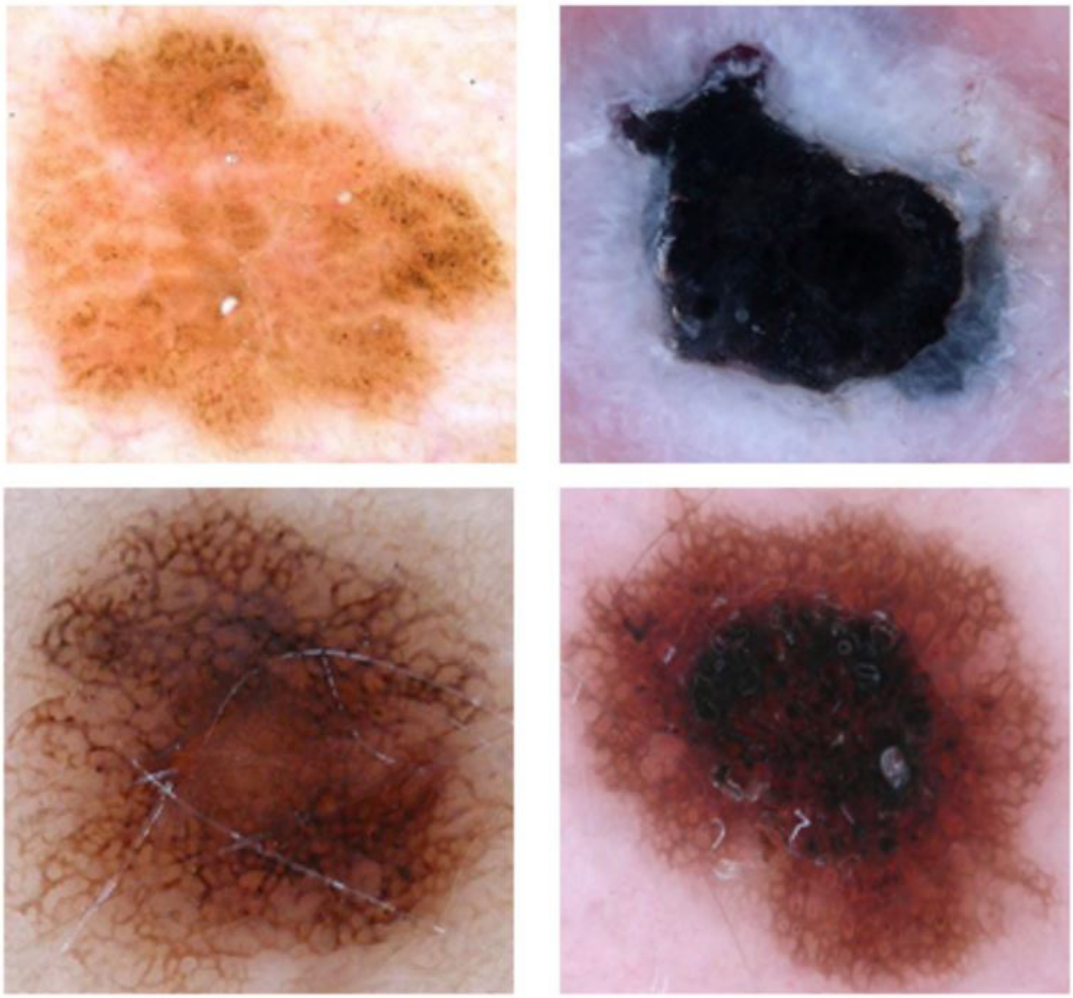

Figure 3. Examples of dermoscopic images with detection error.

The reticular pattern is one of these features, and the contribution for the accurate identification with automatic methodologies by using digital imaging methods, rationalizes this work. Moreover, the proposed method avoids usual preprocessing steps, being suited for its use with different acquisition systems after a simple cropping image operation. In fact, the approach presented in this work does not use lesion segmentation or artifact removal as a preprocessing step. Instead, as the main goal is the detection of reticular pattern, the cropped image encompassed lesion and also surrounding skin. In the particular case of reticular pattern detection, there are several cases where this structure emerges outside the formal segmentation of the lesion (whose border is artificial imposed by segmentation rules). The reticular pattern (particularly in the lesion border) is often neglected by the segmentation procedures, as it vanishes outside the pigmented structure in a subtle way. Therefore, a novel approach (rapid, robust and presenting low complexity) is introduced for reticular pattern identification using a Curvelet Transform.

Experimental results from a set of lesions obtained from three different databases (as presented before) shows that the algorithm achieves good detection scores with a simple group of features (standard deviation, entropy and energy), extracted from the image sub-band decomposition. Hence, the method can be regarded as a valuable tool in a dermoscopy analysis system.

The evaluation metrics are the standard for assess the classifier performance. In the present work, as is possible to observe in Table 1, evaluation metrics (SE, SP and Q) are 82.35, 76.79 and 80.38 respectively. As referred in the introduction section, there are other works addressing this issue of reticular pattern, however the majority use lesion segmentation as a preprocessing step, and some fail to indicate all evaluation metrics. Thus, compare the proposed methodology with works with similar goals (but different methods and metrics) is a demanding task. Even so, being the reticular pattern (detection, identification or characterization) the main goal of all works, it is worth to look for ways to comparison, among the offered information. Concerning accuracy, Anantha et al. (2004) obtained 80% and Sadeghi et al. (2011) 93%. In contrast, in Leo et al. (2010), regarding atypical network, the accuracy values were not shown, but Sensitivity and Specificity are 80% and 82% respectively. Also, in view of the difficulty in comparing results, and adding clinical concerns, the number of true positives can be regarded as the strongest indicator. Therefore, sensitivity values can be considered as the first value for comparison (when is lacking complete information for others), whose values averaged 82.35% in this work.

Despite the results of the SE present themselves as promising, it is possible to find some "difficult" images as is shown in Figure 3, thus tricking the classifier. These images are challenging, as they possess other textured base dermoscopic structures, whose presence confounds the classifier.

To overcame this problem and hence improve these results, the reticular pattern criteria detection should include other predictable properties (behind texture based features) in these structures, such as dots, pigment color, background color and spatial organization of holes. Afterwards, an automatic classifier can be trained using this additional information, to refine the final decision criteria. This approach is now being tested and results will be presented in the near future. Future work should also focus on a detailed evaluation of the proposed algorithm in a larger database, and in the characterization of the detected reticular pattern in order to discriminate typical from atypical patterns, which is an important inkling to perceive malignant lesions.

Acknowledgements

This work was co-funded by DERMCALSS, CENTRO-07-ST24-FEDER-002022, and PEst-OE/EEI/LA0008/2013.

References

Anantha M, Moss R, Stoecker W. Detection of pigment network in dermatoscopy images using texture analysis. Computerized Medical Imaging and Graphics. 2004; 28(5):225-34. http://dx.doi.org/10.1016/j.compmedimag.2004.04.002. PMid:15249068.

Arroyo JG, Zapirain BG. Detection of pigment network in dermoscopy images using supervised machine learning and structural analysis. Computers in Biology and Medicine. 2014; 44:144-57. http://dx.doi.org/10.1016/j.compbiomed.2013.11.002. PMid:24314859.

Barata C, Marques J, Rozeira J. A system for the detection of pigment network in dermoscopy images using directional filters. IEEE Transactions on Biomedical Engineering. 2012; 59(10):2744-54. http://dx.doi.org/10.1109/TBME.2012.2209423. PMid:22829364.

Baumert J, Schmidt M, Giehl KA, Volkenandt M, Plewig G, Wendtner C, Schmid-Wendtner MH. Time trends in tumour thickness vary in subgroups: analysis of 6475 patients by age, tumour site and melanoma subtype. Melanoma Research. 2009; 19(1):24-30. http://dx.doi.org/10.1097/CMR.0b013e32831c6fe7. PMid:19430403.

Benelli C, Roscetti E, Pozzo VD, Gasparini G, Cavicchini S. The dermoscopic versus the clinical diagnosis of melanoma.

European Journal of Dermatology. 1999; 9(6):470-6. PMid:10491506.

Betta G, Di Leo G, Fabbrocini G, Paolillo A, Sommella P. Dermoscopic image-analysis system: Estimation of atypical pigment network and atypical vascular pattern. In: Proceedings of the IEEE International Workshop on Medical Measurement and Applications (MeMea 2006); 2006 Apr 20-21; Benevento, Italy. Washington: IEEE; 2006. p. 63-7. http://dx.doi.org/10.1109/MEMEA.2006.1644462.

Bleyer A, Viny A, Barr R. Cancer in 15- to 29-year-olds by primary site. The Oncologist. 2006; 11(6):590-601. http://dx.doi.org/10.1634/theoncologist.11-6-590. PMid:16794238.

Calderbank A, Daubechies I, Sweldens W, Yeo BL. Lossless image compression using integer to integer Wavelet Transforms. In: Proceedings of the International Conference on Image Processing; 1997 Oct 26-29; Santa Barbara, CA, USA. Washington: IEEE; 1997. p. 596-9. http://dx.doi.org/10.1109/ICIP.1997.647983.

Candès E, Demanet L, Donoho DL, Ying L. Fast discrete curvelet transforms. Multiscale Modeling & Simulation. 2006; 5(3):861-99. http://dx.doi.org/10.1137/05064182X.

Candès J. Ridgelets: theory and applications [thesis]. Stanford: Department of Statistics, Stanford University; 1998.

Do MN, Vetterli M. The Finite Ridgelet Transform for image representation. IEEE Transactions on Image Processing. 2003; 12(1):16-28. http://dx.doi.org/10.1109/TIP.2002.806252. PMid:18237876.

Downing A, Newton-Bishop J, Forman D. Recent trends in cutaneous malignant melanoma in the Yorkshire region of England; incidence, mortality and survival in relation to stage of disease, 1993-2003. British Journal of Cancer. 2006; 95(1):91-5. http://dx.doi.org/10.1038/sj.bjc.6603216. PMid:16755289.

Eltoukhy MM, Faye I, Samir BB. Breast cancer diagnosis in digital mammogram using multiscale curvelet transform. Computerized Medical Imaging and Graphics. 2010; 34(4):269-76. http://dx.doi.org/10.1016/j.compmedimag.2009.11.002. PMid:20004076.

Fadili MJ, Starck JL. Curvelets and Ridgelets. In: Meyers R, editor. Encyclopedia of complexity and system science. New York: Springer; 2007.

Ferlay F, Steliarova-Foucher E, Lortet-Tieulent J, Rosso S, Coebergh JW, Comber H, Forman D, Bray F. Cancer incidence and mortality patterns in Europe: estimates for 40 countries in 2012. European Journal of Cancer. 2013; 49(6):1374-403. http://dx.doi.org/10.1016/j.ejca.2012.12.027. PMid:23485231.

Fleming M, Steger C, Zhang J, Gao J, Cognetta A, Pollak I, Dyer C. Techniques for a structural analysis of dermatoscopic imagery. Computerized Medical Imaging and Graphics. 1998; 22(5):375-89. http://dx.doi.org/10.1016/S0895-6111(98)00048-2. PMid:9890182.

Fonseca-Pinto R, Caseiro P, Andrade A. Image Empirical Mode Decomposition (IEMD) in dermoscopic images: Artefact removal and lesion border detection. In: Proceedings of the Signal Processing Patterns Recognition and Applications (SPPRA 2010); 2010 Feb 17-19; Innsbruck, Austria. Canada: IASTED; 2010. p. 341-5.

Friedman RJ, Rigel DS, Kopf AW. Early detection of malignant melanoma: the role of the physician examination and self examination of the skin. CA: A Cancer Journal for Clinicians. 1985; 35(3):130-51. http://dx.doi.org/10.3322/canjclin.35.3.130. PMid:3921200.

Gardezi JS, Faye I, Eltoukhy MM. Analysis of mammogram images based on texture features of curvelet Sub-bands. In: Proceedings of the ICGIP 2013: Fifth International Conference on Graphic and Image Processing; 2013 Oct 26; Hong Kong, China. Washington: IEEE; 2014. v. 906924. http://dx.doi.org/10.1117/12.2054183.

Grana C, Cucchiara R, Pellacani G, Seidenari S. Line detection and texture characterization of network patterns. In: Proceedings of the ICPR'06: 18th International Conference on Pattern Recognition; 2006; Hong Kong, China. Washington: IEEE; 2006. p. 275-8. v. 2.

Leo GD, Paolillo A, Sommella P, Fabbrocini G. Automatic diagnosis of melanoma: a software system based on the 7-point checklist. In: Proceedings of the HICSS 2010: 43rd Hawaii International Conference on System Sciences; 2010 Jan 5-8; Honolulu, HI, USA. Washington: IEEE; 2010. p. 1-10. http://dx.doi.org/10.1109/HICSS.2010.76.

Li B, Meng MQH. Texture analysis for ulcer detection in capsule endoscopy images. Image and Vision Computing. 2009; 27(9):1336-42. http://dx.doi.org/10.1016/j.imavis.2008.12.003.

Liu W, Hill D, Gibbs A, Tempany M, Howe C, Borland R, Morand M, Kelly J. What features do patients notice that help to distinguish between benign pigmented lesions and melanomas? The ABCD(E) rule versus the seven-point checklist. Melanoma Research. 2005; 15(6):549-54. http://dx.doi.org/10.1097/00008390-200512000-00011. PMid:16314742.

Longo DL, Fauci AS, Kasper DL, Hauser SL, Jameson JL, Loscalzo J. Harrison's principles of internal medicine. 18th ed. New York: McGraw-Hill; 2012.

Menzies SW, Ingvar C, McCarthy WH. A sensitivity and specificity analysis of the surface microscopy features of invasive melanoma. Melanoma Research. 1996; 6(1):55-62. http://dx.doi.org/10.1097/00008390-199602000-00008. PMid:8640071.

Menzies SW. A method for the diagnosis of primary cutaneous melanoma using surface microscopy. Dermatologic Clinics. 2001; 19(2):299-305, viii. http://dx.doi.org/10.1016/S0733-8635(05)70267-9. PMid:11556238.

Nikam SB, Agarwal S. Fingerprint liveness detection using curvet energy and cooccurrence signatures. In: Proceedings of the CGIV '08: Fifth International Conference on Computer Graphics, Imaging and Visualization; 2008 Aug 26-28; Penang, Malaysia. Washington: IEEE; 2008. p. 217-22. http://dx.doi.org/10.1109/CGIV.2008.9.

Paradiso MA, Carney T. Orientation discrimination as a function of stimulus eccentricity and size: Nasal/temporal retinal asymmetry. Vision Research. 1988; 28(8):867-74. http://dx.doi.org/10.1016/0042-6989(88)90096-X. PMid:3250082.

Rogers HW, Weinstock MA, Harris AR, Hinckley MR, Feldman SR, Fleischer AB, Coldiron BM. Incidence estimate of nonmelanoma skin cancer in the United States, 2006. Archives of Dermatology. 2010; 146(3):283-7. http://dx.doi.org/10.1001/archdermatol.2010.19. PMid:20231499.

Sadeghi M, Razmara M, Lee TK, Atkins MS. A novel method for detection of pigment network in dermoscopic images using graphs. Computerized Medical Imaging and Graphics. 2011; 35(2):137-43. http://dx.doi.org/10.1016/j.compmedimag.2010.07.002. PMid:20724109.

Sant M, Allemani C, Santaquilani M, Knijn A, Marchesi F, Capocaccia R. EUROCARE-4. Survival of cancer patients diagnosed in 1995-1999. Results and commentary. European Journal of Cancer. 2009; 45(6):931-91. http://dx.doi.org/10.1016/j.ejca.2008.11.018. PMid:19171476.

Soyer HP, Smolle J, Leitinger G, Rieger E, Kerl H. Diagnostic reliability of dermoscopic criteria for detecting malignant melanoma. Dermatology. 1995; 190(1):25-30. http://dx.doi.org/10.1159/000246629. PMid:7894091.

Starck JL, Candès E, Donoho DL. The curvelet transform for image denoising. IEEE Transactions on Image Processing. 2002; 11(6):670-84. http://dx.doi.org/10.1109/TIP.2002.1014998. PMid:18244665.

Stern RS. Prevalence of a history of skin cancer in 2007: results of an incidence-based model. Archives of Dermatology. 2010; 146(3):279-82. http://dx.doi.org/10.1001/archdermatol.2010.4. PMid:20231498.

Sumana IJ. Image retrieval using discrete curvelet [dissertation]. Melbourne: Gippsland School of Information Technology, Monash University; 2008.

Viola P, Jones MJ. Robust real-time face detection. International Journal of Computer Vision. 2004; 57(2):137-54. http://dx.doi.org/10.1023/B:VISI.0000013087.49260.fb.

Authors

Marlene Machado[1], Jorge Pereira[1], Rui Fonseca-Pinto[1,2]*

[1] Multimedia Signal Processing Group, Instituto de Telecomunicações, Campus 2, IPLeiria, 2411-901, Leiria, Portugal.

[2] School of Technology and Management, Polytechnic Institute of Leiria, Leiria, Portugal.